ResearchGate

See discussions, stats, and author profiles for this publication at: https://www.researchgate.net/publication/51058656

Molecular Dynamics Study of Effects of Temperature and Concentration on Hydrogen-Bond Abilities of Ethylene Glycol and Glycerol: Implications for Cryopreservation

ARTICLE *in* THE JOURNAL OF PHYSICAL CHEMISTRY A · MAY 2011

Impact Factor: 2.69 · DOI: 10.1021/jp111162w · Source: PubMed

CITATIONS
23

READS
30

4 AUTHORS, INCLUDING:

Lindong Weng
Massachusetts General Hospital
28 PUBLICATIONS **112** CITATIONS
SEE PROFILE

Cong Chen
Dalian University of Technology
30 PUBLICATIONS **161** CITATIONS
SEE PROFILE

Weizhong Li
Dalian University of Technology
98 PUBLICATIONS **538** CITATIONS
SEE PROFILE

Available from: Lindong Weng
Retrieved on: 25 January 2016

THE JOURNAL OF PHYSICAL CHEMISTRY A

ARTICLE

pubs.acs.org/JPCA

Molecular Dynamics Study of Effects of Temperature and Concentration on Hydrogen-Bond Abilities of Ethylene Glycol and Glycerol: Implications for Cryopreservation

Lindong Weng, Cong Chen, Jianguo Zuo, and Weizhong Li*

Key Laboratory of Ocean Energy Utilization and Energy Conservation of Ministry of Education, Dalian University of Technology, Dalian, Liaoning Province, People's Republic of China, 116024

Supporting Information

ABSTRACT: The state of intracellular water is important in all phases of cryopreservation. Intracellular water can be transported out of the cell, transferred into its solid phase, or blocked by cryoprotectants and proteins in the cytoplasm. The purpose of the present study is to determine the amount of hydrogen-bonded water in aqueous ethylene glycol and glycerol solutions. The effects of temperature and concentration on the density and the hydrogen bonding characteristics of the solution are evaluated quantitatively in this study. To achieve these aims, a series of molecular dynamics simulations of ethylene glycol/water and glycerol/water mixtures of molalities ranging from 1 to 5 m are conducted at 1 atm and at 273, 285, and 298 K, respectively. The simulation results show that temperature and concentration have variable effects on solution density. The proportion of the hydrogen-bonded water by solute molecules increases with rising molality. The ability of the solute molecules to hydrogen bond with water molecules weakens as the solution becomes more concentrated. Moreover, it turns out that the solution concentration can influence the hydrogen bonding characteristics more greatly than the temperature. The glycerol molecule should be a stronger "water blocker" than the ethylene glycol molecule corresponding to the same conditions. These findings provide insight into the cryoprotective mechanisms of ethylene glycol and glycerol in aqueous solutions, which will confer benefits on the cryopreservation.

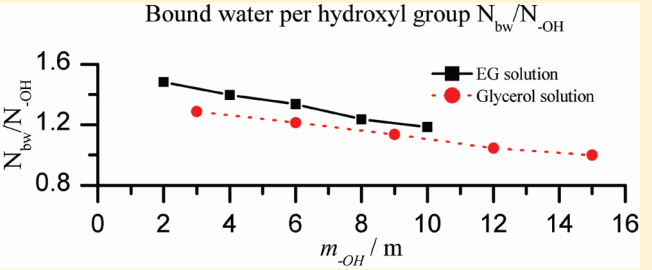

1. INTRODUCTION

Intracellular water is categorized into three parts in cryobiology: the water lost by the cell during freezing, that participating in intracellular ice formation (IIF) and intracellular ice growth (IIG), and that bound by cryoprotective agents (CPAs) and cytoplasmic proteins through hydrogen bonds (H-bonds) or other interactions. Cryobiologists have great interest in analyzing these roles of intracellular water, both qualitatively and quantitatively, and several theories have been tested with experiments.

The model for calculating water loss from cells subjected to freezing for cryopreservation first was proposed by Mazur[1] in 1963, but other more improved models have emerged.[2] For instance, Elliott et al.[3−6] investigated the osmotic behavior of various cryoprotective solutions based on the osmotic virial equations. Cryomicroscopy and a differential scanning calorimeter (DSC) also have been employed to directly measure and indirectly calculate the volumetric response of cells during freezing,[7−9] while electronic particle counters can predict the change of the cellular volume during the equilibrium freezing protocol.[10] Other laboratories have studied ice formation and growth. Toner et al.[11] applied thermodynamic and kinetic theories to prescribe the surface-catalyzed nucleation and the volume-catalyzed nucleation in the cytoplasm during freezing. Karlsson and Cravalho[12] expanded the theory proposed by Toner et al.[11] and developed a model to predict the diffusion-limited crystal growth inside biological cells during freezing. The experimental approaches such as cryomicroscopy and DSC were also used to study the characteristics of IIF and IIG.[13−16]

However, the water restricted by solutes like CPAs and cytoplasmic proteins has received less investigation for two reasons. First, the content of bound water is brought into a constant V_b in the above models when calculating the water loss, IIF and IIG. The bound water in the osmotically inactive volume V_b comes from blockage by solutes such as CPAs, cytoplasmic proteins, and other large molecules. The value of the content of bound water is not considered in these models because V_b has well-accepted values relevant to many cell types. Second, the technical difficulty of macroscopic approaches in cryobiological investigations of bound water impedes a simple study.[6]

Nonetheless, the bound water and its inherent formation mechanisms have far-reaching implications for cryopreservation.[17,18] At the same time, microscopic approaches such as molecular dynamics

Received: November 23, 2010
Revised: March 30, 2011
Published: April 18, 2011

ACS Publications © 2011 American Chemical Society

(MD) simulation may enable both the calculation of bound water and the exploration of molecular mechanisms determining it. MD simulation has become a useful tool for investigating biomolecules, complementary to experiments.[19] Plenty of MD simulations have been applied to investigate CPA solutions, which treated their cryoprotective properties as either the main aim or a byproduct of the simulation.

Both the structure and characteristics of H-bonding of aqueous solutions of dimethyl sulphoxide[20] and methanol and ethanol[21] were investigated. It was pointed out that dimethyl sulphoxide typically formed two H-bonds with water molecules.[20] The responses of water and methanol to electronic polarization were researched by both density functional theory and a polarizable force field based on the chemical potential equalization principle.[22] MD studies[23,24] of sodium chloride solutions in methanol/water mixtures have focused primarily on aspects of structure, preferential solvation of ions, and H-bonding network. It was found that cations and anions were preferentially solvated by methanol molecules in the methanol-deficient mixture.[23] Other studies[25,26] were undertaken to investigate glycerol in the crystal, glass, and liquid phases at the molecular level. The conformational distribution of glycerol was also studied by density functional theory, and the strong similarity of the experimental spectra of the gas and of the liquid in the 750−1600 cm^{-1} spectral region implied that the conformational composition of the liquid was similar to that of the gas phase.[27] The structural and dynamical properties of liquid glycerol[28] and the cryoprotective properties of glycerol/water mixtures[29] were studied by MD simulations. Researchers[30] employed MD simulation to predict the glass-transition temperature of glycerol/water binary systems. After that, H-bonding characteristics of cryoprotective media such as glycerol/water and glycerol/sodium chloride/water mixtures were investigated in depth.[31−33]

The hydrogen bond is one of the most important mechanisms underlying the blockage of intracellular water and is critical in cryobiology,[17] but there have been minimal calculations of the H-bonded water content in CPA solutions. Based on our current observations, MD studies are rarely targeted to the cryoprotective properties of ethylene glycol (EG) in aqueous solutions.[34] Moreover, the effects of temperature and concentration on the ability of the CPA molecule to H-bond with water molecules have not been evaluated quantitatively. In the present study, MD simulations of aqueous EG and glycerol solutions are undertaken using an isothermal−isobaric ensemble because EG and glycerol hold great promise for cryopreservation in virtue of their excellent cryoprotective properties.[35−38] Our quantitative evaluations of the effects of temperature and concentration on both the density and the H-bonding characteristics of the solution are presented with the hope that this information can broaden our microscopic understanding of the protective mechanisms of EG and glycerol in aqueous solutions.

Hereafter, the term "bound water" refers in particular to the water that forms H-bonds with the solute molecule, namely, the H-bonded water. The H-bonded water can participate in the water loss, IIF, or IIG considerably harder than water with no solute−solvent interactions.

2. METHODS

2.1. MD Simulation Methods. Simulations in this study are conducted by means of the MD simulation package NAMD[39] (version 2.7b3) using the all-atom CHARMM22 force field. The force-field parameter sets for EG and glycerol molecules come from the work by Reiling et al.[40] which reparameterized the CHARMM22 force field for carbohydrates. The TIP3P[41] water model is employed as solvent in the simulation box.

Table 1. Compositions of the Simulation Boxes of Aqueous EG Solutions of Molalities *m* Ranging from 1 to 5 m[a]

box	*m* (m)	*x* (%)	N_e	N_w
e-1	1	5.8	45	2498
e-2	2	11.0	72	1997
e-3	3	15.7	108	1995
e-4	4	19.9	72	1009
e-5	5	23.7	90	991

[a] *x* is mass fraction of EG; N_e number of EG molecules; N_w number of water molecules.

Table 2. Compositions of the Simulation Boxes of Aqueous Glycerol Solutions of Molalities *m* Ranging from 1 to 5 m[a]

box	*m* (m)	*x* (%)	N_g	N_w
g-1	1	8.4	45	2498
g-2	2	15.6	72	2009
g-3	3	21.6	108	2000
g-4	4	26.9	72	994
g-5	5	31.5	90	993

[a] *x* is mass fraction of glycerol; N_g number of glycerol molecules; N_w number of water molecules.

The isothermal−isobaric (NPT) ensemble is used so that temperature *T*, pressure *P*, and the number of molecules *N* are fixed. The simulation boxes are set up to produce the commonly used compositions of the cryoprotective medium. The compositions of these simulation boxes have been reported in Tables 1 and 2.

In our simulations, the pressure is maintained at 1 atm, and the temperature is fixed at 273, 285, and 298 K, respectively. Such a temperature range of 25 K is determined for two reasons: (1) Most of the variables in the well-established cryobiological theories like V_b and the latent heat of fusion ΔH_f are parametrized in the temperature range of 273−298 K. Hence, simulation results obtained at 273, 285, and 298 K should be useful complements to the existing theories. (2) Comparisons of MD results of different concentrations at a given temperature are necessary in this study. Therefore, the temperature must be kept above 273 K to avoid the possible occurrence of the ice crystallization in the solutions of low molalities. This temperature range can ensure the evaluation validity.

The parameters configuring the simulation procedures are reported below.

The distance beyond which electrostatic and van der Waals interactions are truncated is 12 Å. When the distance is beyond 10 Å, the switching functions begin to take effect to smoothly reduce electrostatic and van der Waals interactions to zero. The time step is 2 fs. The SHAKE algorithm[42] is used to fix the vibrations of the fastest atoms. Specifically, the hydrogen−oxygen and hydrogen−hydrogen positions in waters are constrained to the nominal length or angle and the bond between each hydrogen atom and the atom to which it is bonded is similarly constrained. The temperature is fixed using Langevin dynamics[43] with a damping coefficient of 5 ps^{-1}. The pressure is fixed by a

modified Nosé-Hoover method,[44] which is a combination of the constant pressure algorithm proposed by Martyna et al.[45] with piston fluctuation control implemented using Langevin dynamics.[46] Periodic boundary conditions are applied and the Particle Mesh Ewald (PME) method[47] is employed with a grid spacing of about 1.0 Å. The PME interpolation order is cubic and the direct sum tolerance is 10^{-6}. Initial velocities are generated randomly from a Gaussian distribution. The above-mentioned parameters configuring our simulation are specified by referring to the NAMD user's guide.[44] A first run for 20 ps is conducted to minimize the energy of the system and then a fully equilibrium for 2.5 ns is operated. Finally, another run for 2.5 ns is repeated for the statistic calculation.

The long period of simulation (more than 5 ns) can realize the complete equilibrium of the system in this study. The values of the total, potential, and kinetic energies of the system can insignificantly fluctuate around certain values after about 100 ps. To illustrate this point, the changes of the total, potential, and kinetic energies of 3 m aqueous EG solution at 298 K during the simulation period are presented as an example in the Supporting Information.

All MD simulations are performed on a SGI Altix XE 1300 Linux Computing Cluster (Silicon Graphics International, Landing Parkway Fremont, CA) at School of Energy and Power Engineering of Dalian University of Technology.

2.2. Definition of H-Bond and Values of the Geometric Criteria. The hydrogen bond can be determined according to either energetic or geometric criteria.[21,48] The geometric criteria are employed in this study so that detailed information on atoms constituting the H-bond can be obtained.

There are two types of H-bonds in aqueous EG and glycerol solutions: the strong O−H···O H-bond and the weak C−H···O one because both carbon and oxygen atoms are electronegative and able to attract hydrogen atoms. Even if the C−H···O H-bond should be widespread, many questions concerning such a weak H-bond still exist and it may not be able to be identified in many cases.[49] It was discovered by Chelli et al.[50] that the number of C−H···O H-bonds per molecule was much smaller than that of O−H···O in the liquid formic acid. The recent research by Chen et al.[31] also proved the absence of the weak C−H···O H-bond in the aqueous glycerol solution. These findings encourage the present study to solely take the strong O−H···O H-bond into consideration.

The geometric criteria can be explained in detail as follows and a graphical explanation has been presented in Figure 1: (1) The distance between the donor and the acceptor oxygen atoms R_{OO} is smaller than R_{OO}^{C}; (2) The distance between the acceptor oxygen atom and the hydrogen atom involved in the H-bond R_{OH} is smaller than R_{OH}^{C}; (3) The angle of H−O···O φ is smaller than φ^{C}.

The positions of the first minima of the radial distribution functions $g_{OO}(r)$ and $g_{OH}(r)$ are determined as the cutoff distances R_{OO}^{C} and R_{OH}^{C}, respectively. The values for $g_{OO}(r)$ and $g_{OH}(r)$ of all the simulation systems in this study are quantitatively similar. Therefore, it is reasonable to use the same distance criteria for EG/water and glycerol/water mixtures. According to the $g_{OO}(r)$ and $g_{OH}(r)$ calculated in this study (not presented in this paper for briefness), the values of R_{OO}^{C} and R_{OH}^{C} are 3.5 and 2.45 Å, respectively. The values of R_{OO}^{C} and R_{OH}^{C} obtained in our study are similar to those reported in previous studies.[21,26,51−55] With regard to the critical angle φ^{C}, the distribution of the angles of all the pairs of oxygen atoms that satisfy criteria (1) and (2), which are not presented in this paper for briefness, indicates that only a negligibly small proportion of the total pairs have a φ larger than 30°. Therefore, φ^{C} is equal to 30° in our study.

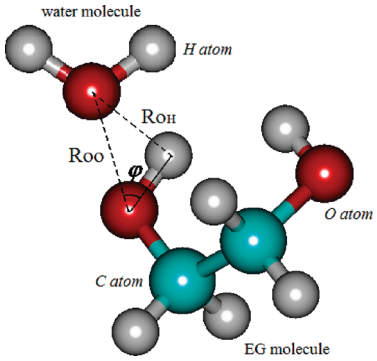

Figure 1. Graphical explanation of the geometric definition of the EG−water H-bond.

2.3. Quantitative Evaluation of the Ability of the Solute Molecule to Form H-Bonds with Water Molecules. The ability of the solute molecule to form H-bonds with water molecules is evaluated by two criteria: the mass fraction of the bound water out of the total water W_{bw}/W_w and the number of bound water molecules by one solute molecule N_{bw}/N_s. In the statistic calculation, the water molecule that forms one or more H-bonds with solute molecules is determined as one bound (or H-bonded) water molecule.

To quantify the effects of temperature and concentration on N_{bw}/N_s, eq 1 is proposed to establish the relationship between N_{bw}/N_s and m.

$$\frac{N_{bw}}{N_s} = a_1 + b_1 \cdot m \tag{1}$$

where N_{bw} is the number of the bound water molecules, N_s is the number of the solute molecules, and a_1 and b_1 are the temperature-dependent fitting parameters.

Further, W_{bw}/W_w can be expressed as follows:

$$\frac{W_{bw}}{W_w} = M_w \cdot \frac{N_{bw}/N_A}{W_w} \tag{2}$$

where W_{bw} is the mass of the bound water in g, W_w is the mass of the total water in g, M_w is the molar mass of water (18 g/mol), and N_A is the Avogadro number (6.02×10^{23} mol^{-1}).

Considering the molality of the solution $m = (N_s/N_A)/(W_w/1000)$,

$$\frac{W_{bw}}{W_w} = \frac{M_w}{1000} \cdot m \cdot \frac{N_{bw}}{N_s} \tag{3}$$

Thereby, W_{bw}/W_w is correlated with m by the following equation.

$$\frac{W_{bw}}{W_w} = a_2 \cdot m + b_2 \cdot m^2 \tag{4}$$

where the parameters $a_2 = a_1 \cdot (M_w/1000)$ and $b_2 = b_1 \cdot (M_w/1000)$.

3. RESULTS AND DISCUSSION

3.1. Density Investigation of Aqueous EG and Glycerol Solutions. The densities of aqueous EG and glycerol solutions ρ

Table 3. Comparison between the Experimental Density ρ_{exp} and the Simulation Result ρ_{sim} of Aqueous EG Solutions of Molalities m[a]

m (m)	ρ_{sim} (g·cm^{-3})	ρ_{exp}[b] (g·cm^{-3})	$(\rho_{sim} - \rho_{exp})/(\rho_{exp}) \times 100$ (%)
1	1.0122	1.006	+0.62
2	1.0136	1.014	−0.04
3	1.0147	1.022	−0.71
4	1.0158	1.028	−1.19
5	1.0165	1.034	−1.69

[a] Ranging from 1 to 5 m at 298 K and 1 atm. [b] The experimental data are given by M. Conde Engineering (at http://www.mrc-eng.com).

Table 4. Comparison between the Experimental Density ρ_{exp} and the Simulation Result ρ_{sim} of Aqueous Glycerol Solutions of Molalities m[a]

m (m)	ρ_{sim} (g·cm^{-3})	ρ_{exp}[b] (g·cm^{-3})	$(\rho_{sim} - \rho_{exp})/(\rho_{exp}) \times 100$ (%)
1	1.0255	1.017	+0.84
2	1.0381	1.034	+0.40
3	1.0491	1.049	+0.01
4	1.0583	1.063	−0.44
5	1.0673	1.075	−0.71

[a] Ranging from 1 to 5 m at 298 K and 1 atm. [b] The experimental data are given by The Dow Chemical Company (at http://www.dow.com).

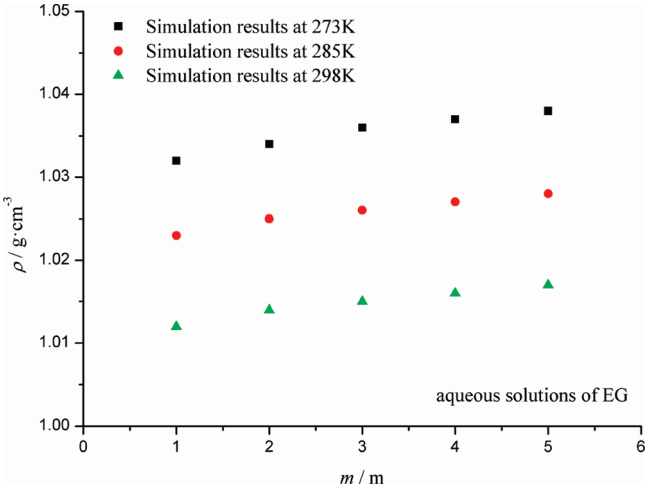

Figure 2. MD simulation results of density ρ of aqueous EG solutions of molalities m ranging from 1 to 5 m at 273, 285, and 298 K.

are statistically calculated based on their compositions and the MD simulation results of their volumes. Comparisons of densities of EG and glycerol solutions at 298 K between the MD simulation and the experimental results are presented in Tables 3 and 4, respectively. The experimental results of the EG and glycerol solutions are given by the public materials provided by M. Conde Engineering[56] and the Dow Chemical Company,[57] respectively. It can be noticed from these tables that the relative error of the simulation result does exist but is acceptable. The simulation results at 273, 285, and 298 K have been graphically displayed in Figures 2 and 3.

On the one hand, the density of the EG solution becomes smaller when the temperature T goes up. When it is heated, the system should undergo a macroscopic expansion because the increasingly intensive motion of molecules can make them depart from each other. On the other hand, the solution becomes denser with a larger molality m. As more solutes are added, the density of the solution grows because the density of the solute is larger than that of the solvent. However, T and m have different effects on the density. As seen in Figure 2, T should be the main factor influencing the density of the EG solution. For instance, the densities of 1 and 5 m EG solutions grow by 1.9 and 2.1%, respectively, with the temperature decrease of 25 K. As for the concentration effect, the densities at 273, 285, and 298 K go up by less than 0.6, 0.5, and 0.5%, respectively, as the molality ascends from 1 to 5 m.

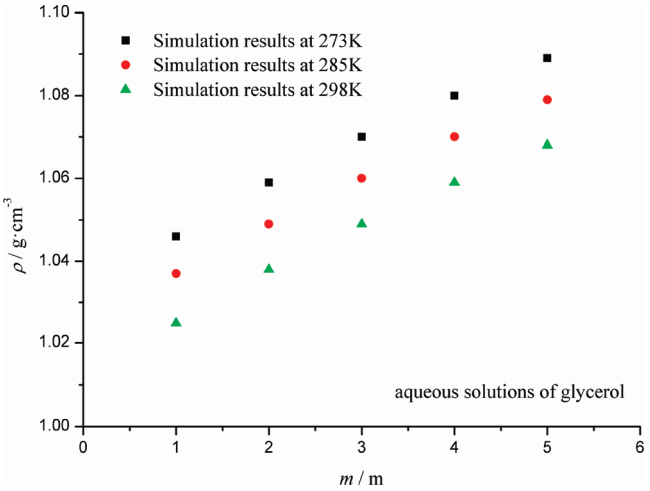

Figure 3. MD simulation results of density ρ of aqueous glycerol solutions of molalities m ranging from 1 to 5 m at 273, 285, and 298 K.

As illustrated in Figure 3, similar trends of $\rho \sim T$ and $\rho \sim m$ are observed for the glycerol solutions. The temperature affects the densities of both EG and glycerol solutions quantitatively similarly. Specifically, the temperature rise of 25 K leads to a decrease in the value of the density by around 2.0%. But, in contrast with the situation of the EG solution, the density of the glycerol solution is mainly affected by m rather than T. The densities of glycerol solutions at 273, 285, and 298 K increase by 4.1, 4.1, and 4.2%, respectively, as the molality rises from 1 to 5 m. But the density of 5 m glycerol solution at 273 K is only 1.9% larger than that at 298 K.

The concentration can affect the density of the EG solution less greatly than that of the glycerol solution. This phenomenon can be attributed to two facts. First, the density of the neat liquid EG (e.g., 1.113 g/cm^3 at 298 K) is smaller than that of the neat liquid glycerol (e.g., 1.261 g/cm^3 at 298 K). As a result, the change of the density of the glycerol solution from neat water to neat liquid glycerol progressively should be greater than that of the EG solution. Second, one more hydroxyl group (−OH) in the glycerol molecule can make itself more quantitatively preferable to form H-bonds than the EG molecule. A more extensive existence of H-bonds between solute molecules and between solute and solvent molecules in the glycerol solution than in the EG solution can contribute to such a phenomenon.

3.2. H-Bonding Characteristics of Aqueous EG and Glycerol Solutions. The numbers of H-bonds in aqueous EG and glycerol solutions are statistically calculated according to the geometric criteria, which have been explained earlier. For each

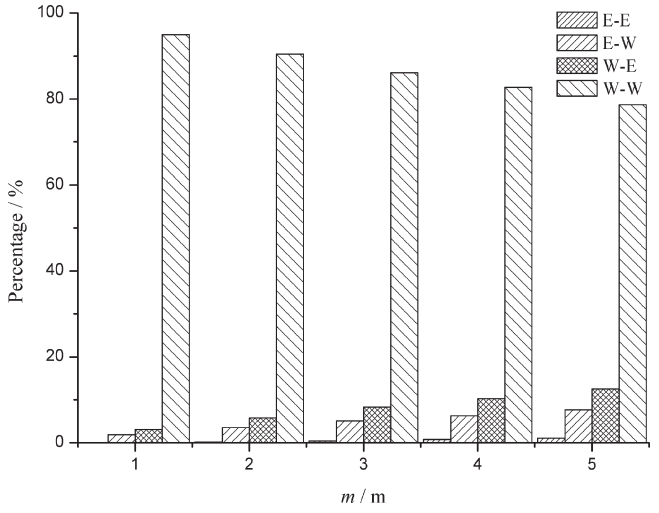

Figure 4. Percentage of each type of H-bond in aqueous EG solutions of molalities *m* ranging from 1 to 5 m at 298 K (E-E: H-bond between EG molecules; E-W: H-bond in which the oxygen atom in the EG molecule is the hydrogen donor and the one in the water molecule is the acceptor; W-E: H-bond in which the oxygen atom in the water molecule is the hydrogen donor and the one in the EG molecule is the acceptor; W-W: H-bond between water molecules.).

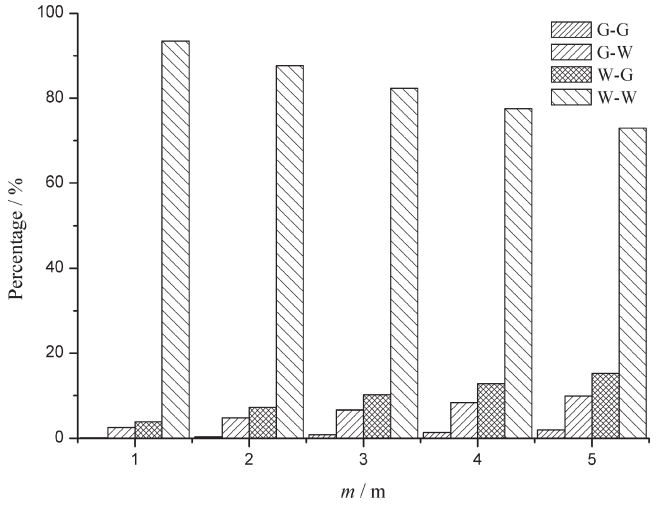

Figure 5. Percentage of each type of H-bond in aqueous glycerol solutions of molalities *m* ranging from 1 to 5 m at 298 K (G-G: H-bond between glycerol molecules; G-W: H-bond in which the oxygen atom in the glycerol molecule is the hydrogen donor and the one in the water molecule is the acceptor; W-G: H-bond in which the oxygen atom in the water molecule is the hydrogen donor and the one in the glycerol molecule is the acceptor; W-W: H-bond between water molecules).

type of H-bond in the solution, the corresponding percentage has been shown in Figures 4 and 5. It is found that the temperature-dependence of the results is marginal so that only the results at 298 K are presented.

Figures 4 and 5 illustrate that, for a given composition, H-bonds between water molecules are dominant among all the H-bonds in the solution. This phenomenon is due to the quantitative advantage of water molecules in the solution. Among all the simulation systems in our study, water molecules are at least 10 times more than solute molecules. Furthermore, the oxygen and hydrogen atoms in the water molecule naturally prefer to attend H-bonds. Such a preference gives birth to the unique physical and chemical properties of the neat water such as its high boiling point. W−W H-bonds account for 95.0∼78.7% of the total amount of H-bonds for the 1−5 m EG solutions and 93.5∼72.9% for the 1−5 m glycerol solutions, respectively.

H-bonds between EG and water molecules account for 5.0%∼20.2% of the population for the 1−5 m EG solutions and those between glycerol and water molecules account for 6.4%∼25.1%, correspondingly. It is also noticed that the percentage of H-bonds formed between the solute molecules is less than 2.0% for all the solutions.

It is attention-attracting that W-E and W-G H-bonds are more abundant than E-W and G-W ones in aqueous EG and glycerol solutions, respectively. Taking 5 m glycerol solution, for instance, 15.2% of the total H-bonds consist of the oxygen atom of the water molecule as the donor of the hydrogen atom and the oxygen atom of the glycerol molecule as the acceptor. On the contrary, H-bonds in which the donor of the hydrogen atom is the oxygen atom of the glycerol molecule only account for 9.9%, 5.3 percentage points less. From the viewpoint of statistical thermodynamics, the different degeneracy of W-E and W-G and E-W and G-W H-bond states can explain the above phenomenon. Generally, one hydrogen atom bound to oxygen can form in average one H-bond, while one oxygen atom, as the hydrogen acceptor, can form two H-bonds simultaneously. Assuming the absence of intramolecular and solute−solute H-bonds, one EG molecule can form two E-W and four W-E H-bonds. In other words, the degeneracy of E-W and W-E H-bond states is 2 and 4, respectively. As for the ideal glycerol solution, the degeneracy of G-W and W-G H-bond states is 3 and 6, respectively. Therefore, the probabilities of W-E and W-G H-bond states can be twice as large as those of E-W and G-W H-bond states, respectively. In our study, it is shown that intramolecular H-bonds in EG and glycerol molecules are hardly noticed. Figures 4 and 5 illustrate the insignificant existence of E-E and G-G H-bonds. As a result, deviations of real EG and glycerol solutions from ideality are minor in terms of the degeneracy of the H-bond state. Therefore, one can conclude that solute molecules can form more H-bonds as the hydrogen acceptor than as the hydrogen donor under the same conditions. Other molecular investigations such as ab initio calculations are necessary to achieve a further energetic analysis, which will be the target of our future work.

Glycerol molecule seems to be more active to form intermolecular H-bonds with its own molecules than EG molecule. The percentage of the G-G H-bonds is 0.1∼2.0% for the 1−5 m glycerol solutions, while the percentage of the E-E H-bonds is 0.1∼1.1% for the 1−5 m EG solutions, as shown in Figures 4 and 5. This phenomenon is because the three hydroxyl groups in the glycerol molecule can enhance the likelihood of solute molecules to interact with each other compared with the situation of the dihydric EG molecule.

The percentage of each type of H-bond except for W-W one increases with a rising molality. This is because solute molecules are more likely to form H-bonds with either water molecules or solute molecules as the solution becomes more concentrated. On the contrary, the percentage of H-bonds between water molecules decreases with a rising molality because more water molecules are captured by solute molecules as more solute molecules exist in the solution.

The temperature effect on the percentage of any type of H-bond can be ignored. Our simulation results show that the differences of percentages at various temperatures are less than

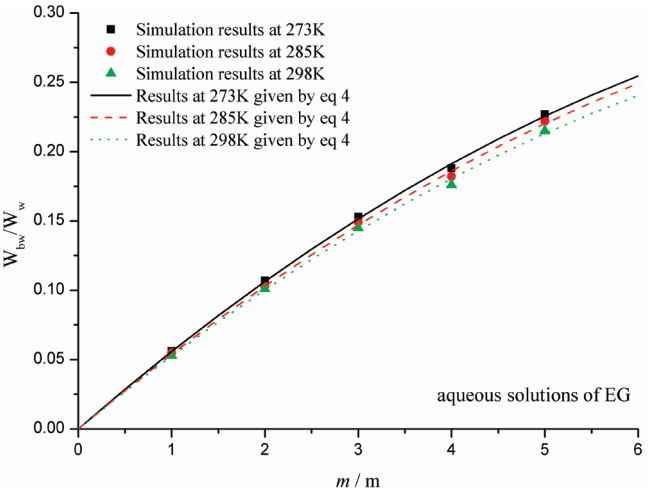

Figure 6. Bound water fraction W_{bw}/W_w of aqueous EG solutions of molalities m ranging from 1 to 5 m at 273, 285, and 298 K.

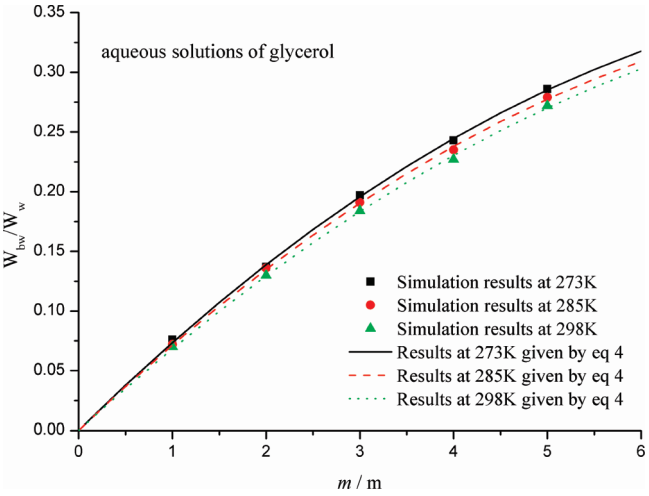

Figure 7. The bound water fraction W_{bw}/W_w of aqueous glycerol solutions of molalities m ranging from 1 to 5 m at 273, 285, and 298 K.

one percentage point and no uniform trends of temperature can be followed. The percentages of all types of H-bonds in EG and glycerol solutions at 273, 285, and 298 K are provided in the Supporting Information. In our opinion, it is the internal factors like the amount of solute molecules that mainly influence the amount of H-bonds. The external factors such as temperature can make minimal influence compared with the concentration.

3.3. Abilities of EG and Glycerol Molecules to H-Bond with Water Molecules and the Relevant Effects of Temperature and Concentration. The relationships between W_{bw}/W_w and m of EG and glycerol solutions have been clearly displayed by the scattered MD simulation results in Figures 6 and 7. The corresponding lines given by eq 4 are also presented.

W_{bw}/W_w increases as the solution becomes more concentrated. In detail, the value of W_{bw}/W_w of the EG solution at 298 K grows more than 3-fold from 5.3 to 21.5% as the molality increases from 1 to 5 m. As for the glycerol solution at 298 K, the corresponding value goes up by 290% from 7.0 to 27.2%. These results show that the bound water content can be affected by the concentration of the solution greatly.

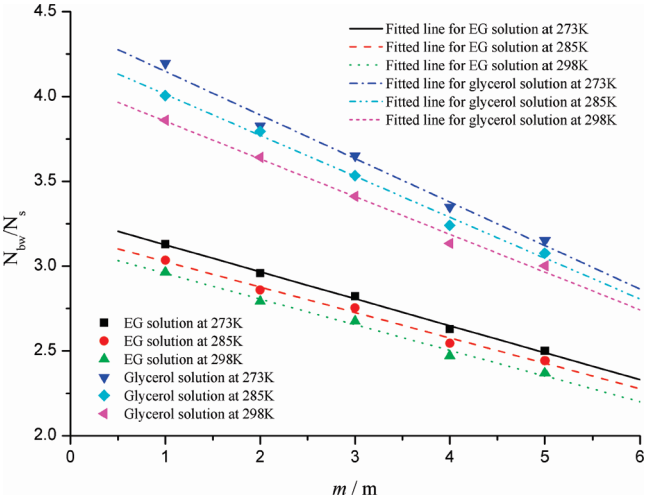

Figure 8. Bound water content per solute molecule N_{bw}/N_s of aqueous EG and glycerol solutions of molalities m ranging from 1 to 5 m at 273, 285, and 298 K.

Another finding is that the temperature does not affect the value of W_{bw}/W_w as obviously as the concentration does. For example, the values of W_{bw}/W_w of the 5 m EG and glycerol solutions decrease by only 5.3 and 4.9%, respectively, as the temperature goes up by 25 K from 273 K.

The above-mentioned findings should be attributed to the fact that the amount of the participants of H-bond (or the amount of the solute molecules) should affect the H-bonding characteristics more greatly than external factors such as temperature. In addition, it should be noticed that, for the bound water content, the temperature range of 25 K may be insufficient to make a significant difference.

The results presented in Figure 8 indicate that N_{bw}/N_s decreases as the molality increases, an opposite trend to $W_{bw}/W_w \sim m$. This trend is because solute molecules are "distracted" to attend the solute−solute H-bonds as the solution becomes more concentrated. This can be confirmed by the fact that the probability of the formation of H-bonds between solute molecules rises when more solute molecules are added. In detail, the percentage of H-bonds between solute molecules in the EG solution at 298 K increases from 0.1 to 1.1% and that in the glycerol solution at 298 K increases from 0.1 to 2.1% when the molality increases from 1 to 5 m. As a result, these increases can result in the decreases in N_{bw}/N_s of 20.1 and 22.2%, correspondingly. Moreover, a decrease in N_{bw}/N_s implies an increase in the amount of H-bonded water molecules per water molecule N_{bw}/N_w because the gain of solute molecules means the loss of water molecules. It was found that the number of glycerol−water H-bonds per water molecule increased with the rising glycerol mole fraction in the study of Dashnau et al.[29] The results in our study have a good agreement with the previous ones[29] for the glycerol solution and prove that the above-mentioned qualitative trends also can be followed by the EG solution.

Compared with the molality, the temperature can affect N_{bw}/N_s insignificantly even if it seems to have a more obvious influence on N_{bw}/N_s than it does on W_{bw}/W_w.

As shown in Figures 6−8, the values of W_{bw}/W_w and N_{bw}/N_s of the glycerol solution are always larger than those of the EG solution according to a given molality and a certain temperature. The different structures of EG and glycerol molecules can lead to

Table 5. Values of the Fitting Parameters a_1 and b_1 in eq 1 and the Corresponding Goodness of Fit R^2 at Various Temperatures T

	EG solution			glycerol solution		
T (K)	a_1	b_1	R^2	a_1	b_1	R^2
273	3.2846	−0.1590	0.9967	4.4042	−0.2566	0.9870
285	3.1762	−0.1498	0.9896	4.2537	−0.2413	0.9935
298	3.1082	−0.1512	0.9913	4.0765	−0.2223	0.9913

Table 6. Values of Parameters a_2 and b_2 in eq 4 at Various Temperatures T

	EG solution		glycerol solution	
T (K)	a_2	b_2	a_2	b_2
273	0.0591	−0.0029	0.0793	−0.0046
285	0.0571	−0.0027	0.0766	−0.0043
298	0.0559	−0.0027	0.0734	−0.0040

such a difference. As discussed earlier, the glycerol molecule is embedded by three hydroxyl groups, whereas EG is a dihydric alcohol, which results in more H-bonded water molecules in the glycerol solution.

The values of the fitting parameters a_1 and b_1 in eq 1 have been listed in Table 5. According to $a_2 = a_1 \cdot (M_w/1000)$ and $b_2 = b_1 \cdot (M_w/1000)$, the values of the parameters a_2 and b_2 in eq 4 are also calculated as listed in Table 6.

3.4. An Investigation of Abilities of EG and Glycerol Molecules to H-Bond with Water Molecules Based on the Hydroxyl Group Molality m_{-OH}. The previous results in this study demonstrate that the amount of the hydroxyl group can significantly influence the ability of the solute molecule to H-bond with water molecules. Therefore, the hydroxyl group molality m_{-OH} is introduced into this study to achieve a deeper analysis. The hydroxyl group molality m_{-OH} of the solution, in m, is defined as the amount of hydroxyl group of the solute in mol in 1 kg water.

The results at 298 K in Figures 6−8 are refined to produce the scattered results in Figures 9 and 10. The results at 273, 285, and 298 K are quantitatively similar because the temperature affects the results marginally. The total trends of W_{bw}/W_w and N_{bw}/N_{-OH} with m_{-OH} are similar with those in Figures 6−8.

To maintain the values of W_{bw}/W_w of EG and glycerol solutions to be equal, the following equation should hold.

$$a_2^e \cdot m_e + b_2^e \cdot m_e^2 = a_2^g \cdot m_g + b_2^g \cdot m_g^2 \quad (5)$$

where m_e and m_g are the molalities of the EG and glycerol solutions, respectively, and a_2^e, b_2^e, a_2^g, and b_2^g are the corresponding parameters in eq 4 for EG and glycerol solutions, respectively.

The relationship between m_e and m_g can be calculated as follows:

$$m_g = \frac{-a_2^g + \sqrt{a_2^{g2} + 4b_2^g \cdot (a_2^e \cdot m_e + b_2^e \cdot m_e^2)}}{2b_2^g} \quad (6)$$

Thereby, the practical relationship between m_e and m_g to generate the same W_{bw}/W_w can be described as eq 6.

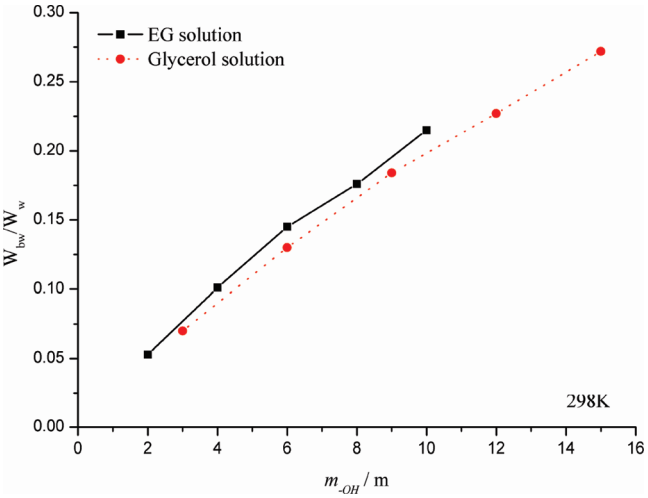

Figure 9. Relationship between the bound water fraction W_{bw}/W_w and the hydroxyl group molality m_{-OH} of aqueous EG and glycerol solutions at 298 K (The lines are just guides to the eye.).

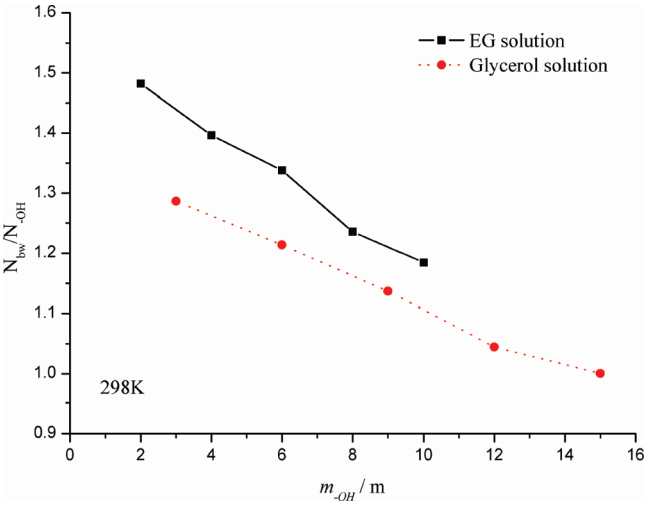

Figure 10. Relationship between the bound water content per hydroxyl group N_{bw}/N_{-OH} and the hydroxyl group molality m_{-OH} of aqueous EG and glycerol solutions at 298 K (The lines are just guides to the eye.).

As for the ideal case, assuming that the abilities of the hydroxyl group of the EG and glycerol molecules are the same, the same m_{-OH}^e and m_{-OH}^g should produce the same W_{bw}/W_w. According to the numbers of the hydroxyl group in the EG and glycerol molecules, the relationship between m_e and m_g to make m_{-OH}^e and m_{-OH}^g equal should be

$$m_g = \frac{2}{3} m_e \quad (7)$$

Thereby, the ideal relationship between m_e and m_g to generate the same W_{bw}/W_w can be described as eq 7. The difference between the ideal and the practical relationships is due to the different amounts of the intermolecular interactions between solute molecules in the EG and glycerol solutions.

In the practical case, more than two-thirds of m_e is needed for m_g to produce the same W_{bw}/W_w according to eq 6, as seen in Figure 11. In other words, m_g (= (2/3)m_e), which makes m_{-OH}^e

dx.doi.org/10.1021/jp111162w |J. Phys. Chem. A 2011, 115, 4729–4737

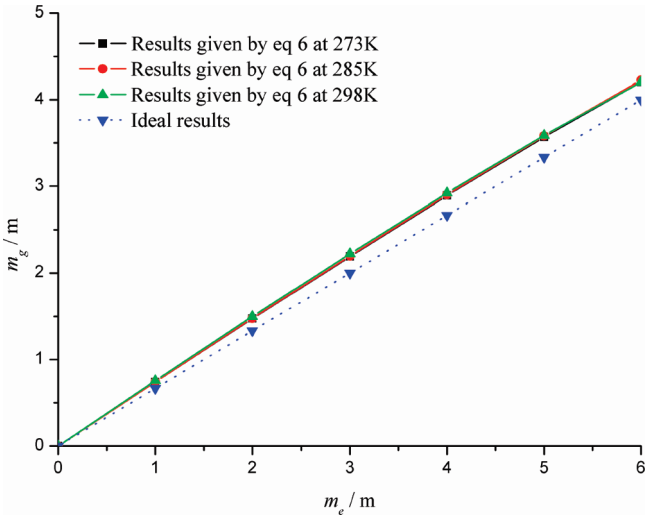

Figure 11. Practical and ideal relationships between m_e and m_g to generate the equal bound water fraction W_{bw}/W_w (The lines are just guides to the eye.).

and $m_{-OH}{}^g$ equal can produce a smaller W_{bw}/W_w than m_e. This phenomenon has been illustrated in Figure 9. Namely, the value of W_{bw}/W_w of the EG solution is slightly greater than that of the glycerol solution corresponding to a given m_{-OH}. This comparison proves that the hydroxyl group of the EG molecule has a greater ability to H-bond with water molecules than that of the glycerol molecule. This phenomenon is also consistent with the trends in Figure 10. The value of N_{bw}/N_{-OH} of the EG solution is greater than that of the glycerol solution corresponding to the same m_{-OH}.

4. CONCLUSIONS

According to the MD simulation results in this study, the densities and the H-bonding characteristics of EG and glycerol solutions have been investigated. The effects of temperature and concentration on these properties have also been quantitatively evaluated. The following conclusions are obtained:

(1) The solution density goes up with either the falling temperature or the rising molality.
(2) The concentration effect on the density of the glycerol solution is greater than the temperature effect, while the case of the EG solution is opposite.
(3) W_{bw}/W_w increases and N_{bw}/N_s decreases with a rising m.
(4) The concentration greatly influences W_{bw}/W_w and N_{bw}/N_s, while the temperature makes insignificant influence.
(5) Glycerol molecule is more active than EG molecule to H-bond with water molecules, while the hydroxyl group of the EG molecule is more active than that of the glycerol molecule.

Quantitative analyses based on eqs 1 and 4 can inform the cryobiologists of the abilities of EG and glycerol to H-bond with water molecules at various temperatures and concentrations. Such information will help to determine the most reasonable composition of the cryoprotective solution according to the concrete requirements of the cryopreservation application. The quantitative findings in this study will benefit our understanding of the protective mechanisms of EG and glycerol in aqueous solutions as well.

■ ASSOCIATED CONTENT

Supporting Information. The changes of the total energy (Figure a), potential energy (Figure b), and kinetic energy (Figure c) of 3 m aqueous EG solution at 298 K during the simulation period, and the percentages of all types of H-bonds in all solutions at various temperatures (Tables a and b). This material is available free of charge via the Internet at http://pubs.acs.org.

■ AUTHOR INFORMATION

Corresponding Author
*Tel.: +86-411-84708774. Fax: +86-411-84708460. E-mail: wzhongli@dlut.edu.cn.

■ ACKNOWLEDGMENT

This work is sponsored by the National Nature Science Foundation of China (50976017) and NSFC's Key Program Projects (50736001). The authors are grateful to Prof. W. Michael Panneton at Saint Louis University for suggestions for improving the language of this paper.

■ REFERENCES

(1) Mazur, P. *J. Gen. Physiol.* **1963**, *47*, 347.
(2) Weng, L.; Li, W.; Zuo, J. *Cryobiology* **2010**, *61*, 194.
(3) Prickett, R. C.; Elliott, J. A. W.; McGann, L. E. *Cryobiology* **2010**, *60*, 30.
(4) Elmoazzen, H. Y.; Elliott, J. A. W.; McGann, L. E. *Biophys. J.* **2009**, *96*, 2559.
(5) Elliott, J. A. W.; Prickett, R. C.; Elmoazzen, H. Y.; Porter, K. R.; McGann, L. E. *J. Phys. Chem. B* **2007**, *111*, 1775.
(6) Prickett, R. C.; Elliott, J. A. W.; Hakda, S.; McGann, L. E. *Cryobiology* **2008**, *57*, 130.
(7) Devireddy, R. V.; Raha, D.; Bischof, J. C. *Cryobiology* **1998**, *36*, 124.
(8) Devireddy, R. V.; Swanlund, D. J.; Roberts, K. P.; Bischof, J. C. *Biol. Reprod.* **1999**, *61*, 764.
(9) Zhang, T.; Isayeva, A.; Adams, S. L.; Rawson, D. M. *Cryobiology* **2005**, *50*, 285.
(10) Zhao, G.; He, L.; Wang, P.; Ding, W.; Xie, X.; Liu, Z.; Zhang, H.; Shu, Z.; Luo, D.; Gao, D. *Chin. Sci. Bull.* **2003**, *48*, 1551.
(11) Toner, M.; Cravalho, E. G.; Karel, M. *J. Appl. Phys.* **1990**, *67*, 1582.
(12) Karlsson, J. O. M.; Cravalho, E. G.; Toner, M. *J. Appl. Phys.* **1994**, *75*, 4442.
(13) Toner, M.; Cravalho, E. G.; Armant, D. R. *J. Membr. Biol.* **1990**, *115*, 261.
(14) Toner, M.; Cravalho, E. G.; Karel, M.; Armant, D. R. *Cryobiology* **1991**, *28*, 55.
(15) Kleinhans, F. W.; Guenther, J. F.; Roberts, D. M.; Mazur, P. *Cryobiology* **2006**, *52*, 128.
(16) Mazur, P.; Pinn, I. L.; Kleinhans, F. W. *Cryobiology* **2007**, *54*, 223.
(17) Franks, F. *Cryobiology* **1983**, *20*, 335.
(18) Storey, K. B.; Baust, J. G.; Buescher, P. *Cryobiology* **1981**, *18*, 315–321.
(19) Hansson, T.; Oostenbrink, C.; van Gunsteren, W. F. *Curr. Opin. Struct. Biol.* **2002**, *12*, 190.
(20) Luzar, A.; Chandler, D. *J. Chem. Phys.* **1993**, *98*, 8160.
(21) Padro, J. A.; Saiz, L.; Guārdia, E. *J. Mol. Struct.* **1997**, *416*, 243.
(22) Chelli, R.; Pagliai, M.; Procacci, P.; Cardini, G.; Schettino, V. *J. Chem. Phys.* **2005**, *122*, 074504.
(23) Hawlicka, E.; Swiatla-Wojcik, D. *Chem. Phys.* **1995**, *195*, 221.

(24) Hawlicka, E.; Swiatla-Wojcik, D. *Chem. Phys.* **1998**, *232*, 361.
(25) Chelli, R.; Procacci, P.; Cardini, G.; Valle, R. G. D.; Califano, S. *Phys. Chem. Chem. Phys.* **1999**, *1*, 871.
(26) Chelli, R.; Procacci, P.; Cardini, G.; Califano, S. *Phys. Chem. Chem. Phys.* **1999**, *1*, 879.
(27) Chelli, R.; Gervasio, F. L.; Gellini, C.; Procacci, P.; Cardini, G.; Schettino, V. *J. Phys. Chem. A* **2000**, *104*, 5351.
(28) Blieck, J.; Affouard, F.; Bordat, P.; Lerbret, A.; Descamps, M. *Chem. Phys.* **2005**, *317*, 253.
(29) Dashnau, J. L.; Nucci, N. V.; Sharp, K. A.; Vanderkooi, J. M. *J. Phys. Chem. B* **2006**, *110*, 13670.
(30) Li, D. X.; Liu, B. L.; Liu, Y.; Chen, C. *Cryobiology* **2008**, *56*, 114.
(31) Chen, C.; Li, W.; Song, Y.; Yang, J. *Mol. Phys.* **2009**, *107*, 673.
(32) Chen, C.; Li, W. Z.; Song, Y. C.; Yang, J. *J. Mol. Liq.* **2009**, *146*, 23.
(33) Chen, C.; Li, W. Z.; Song, Y. C.; Yang, J. *J. Mol. Struct.: THEOCHEM* **2009**, *916*, 37.
(34) Kyrychenko, A.; Dyubko, T. S. *Biophys. Chem.* **2008**, *136*, 23.
(35) Gilmore, J. A.; McGann, L. E.; Liu, J.; Gao, D. Y.; Peter, A. T.; Kleinhans, F. W.; Critser, J. K. *Biol. Reprod.* **1995**, *53*, 985.
(36) Gilmore, J. A.; Liu, J.; Woods, E. J.; Peter, A. T.; Critser, J. K. *Hum. Reprod.* **2000**, *15*, 335.
(37) Fuller, B. J. *Cryo Lett.* **2004**, *25*, 375.
(38) Blanquet, S.; Garrait, G.; Beyssac, E.; Perrier, C.; Denis, S.; Hébrard, G.; Alric, M. *Eur. J. Pharm. Biopharm.* **2005**, *61*, 32.
(39) Phillips, J. C.; Braun, R.; Wang, W.; Gumbart, J.; Tajkhorshid, E.; Villa, E.; Chipot, C.; Skeel, R. D.; Kale, L.; Schulten, K. *J. Comput. Chem.* **2005**, *26*, 1781.
(40) Reiling, S.; Schlenkrich, M.; Brickmann, J. *J. Comput. Chem.* **1996**, *17*, 450.
(41) Jorgensen, W. L.; Chandrasekhar, J.; Madura, J. D.; Impey, R. W.; Klein, M. L. *J. Chem. Phys.* **1983**, *79*, 926.
(42) Ryckaert, J. P. *Mol. Phys.* **1985**, *55*, 549.
(43) Brünger, A. T. *X-PLOR: A system for X-ray Crystallography and NMR*; Yale University Press: New Haven, CT, 1992.
(44) Bhandarkar, M.; Brunner, R.; Chipot, C.; Dalke, A.; Dixit, S.; Grayson, P.; Gullingsrud, J.; Gursoy, A.; Hardy, D.; Humphrey, W. *Urbana* **2003**, *51*, 61801.
(45) Martyna, G. J.; Tobias, D. J.; Klein, M. L. *J. Chem. Phys.* **1994**, *101*, 4177.
(46) Feller, S. E.; Zhang, Y.; Pastor, R. W.; Brooks, B. R. *J. Chem. Phys.* **1995**, *103*, 4613.
(47) Darden, T.; York, D.; Pedersen, L. *J. Chem. Phys.* **1993**, *98*, 10089.
(48) Bertolini, D.; Cassettari, M.; Ferrario, M.; Grigolini, P.; Salvetti, G. *Adv. Chem. Phys.* **1985**, *62*, 277.
(49) Desiraju, G. R. *Acc. Chem. Res.* **1996**, *29*, 441.
(50) Chelli, R.; Righini, R.; Califano, S. *J. Phys. Chem. B* **2005**, *109*, 17006.
(51) De Loof, H.; Nilsson, L.; Rigler, R. *J. Am. Chem. Soc.* **1992**, *114*, 4028.
(52) Root, L. J.; Berne, B. J. *J. Chem. Phys.* **1997**, *107*, 4350.
(53) Guārdia, E.; Marti, J.; Padro, J. A.; Saiz, L.; Komolkin, A. V. *J. Mol. Liq.* **2002**, *96*, 3.
(54) Guārdia, E.; Martí, J.; García-Tarrés, L.; Laria, D. *J. Mol. Liq.* **2005**, *117*, 63.
(55) Nag, A.; Chakraborty, D.; Chandra, A. *J. Chem. Sci.* **2008**, *120*, 71.
(56) *Brine Properties*; M. Conde Engineering: Zurich, Switzerland.
(57) *The Density of Glycerine Solutions*; The Dow Chemical Company: Midland, MI.